Acta Acustica united with Acustica
Vol. 104 (2018) 145 – 152

DOI 10.3813/AAA.919154

Influence of the Lip Horn on Acoustic Pressure Distribution Pattern of Sibilant /s/

Tsukasa Yoshinaga[1)], Annemie Van Hirtum[1,2)], Kazunori Nozaki[3)], Shigeo Wada[1)]

[1)] Graduate School of Engineering Science, Osaka University, 1–3 Machikaneyama, Toyonaka, 560-8531 Osaka, Japan.

[2)] GIPSA-Lab, UMR CNRS 5216, Grenoble Alpes University, 11 rue des Mathématiques (BP46), 38402 Grenoble, France. annemie.vanhirtum@gipsa-lab.grenoble-inp.fr

[3)] Osaka University Dental Hospital, 1–8 Yamadaoka, Suita, 565-0871 Osaka, Japan.

Summary

Influence of the lip horn on the acoustic pressure distribution of the sibilant /s/ was experimentally studied using a vocal tract replica to which a rectangular baffle was added to represent a human face. The sound was generated by a sweep sound source (Frequency: 2–15 kHz) positioned at the inlet of the pharynx or by air flowing through the replica. The sound generated by the sweep source was measured along two semi-circles of radius 4 cm every 2° (near-field) and radius 48 cm every 15° (far-field), where as the sound generated by the flow was measured along semi-circles of radius 10 cm every 2°. From the normalized pressure distributions, it was observed that the lip horn enhances the pressure amplitude up to 15 dB at the center of the lips in both transverse and sagittal plane in the frequency range above 5 kHz. The pressure distribution patterns measured with the acoustic source were similar to those measured with the flow supply. This indicates that the pressure pattern of sibilant /s/ is affected by the vocal tract geometry rather than by the source characteristics.

PACS no. 43.70.-h

1. Introduction

The directivity pattern of sound propagation in human speech has been investigated by several researchers [1, 2, 3]. Monson *et al*. [3] measured the directivity pattern in the transverse plane using a circular microphone antenna (with a radius of 60 cm) equipped with 13 microphones equally spaced by angle 15°. Octave band analysis showed the larger differences in the directivity pattern at the frequencies above 4 kHz compare to those below 4 kHz. Among fricative consonants, sibilant /s/ exhibited the maximum difference in the pressure amplitude (over 10 dB above 8 kHz) between the center and 90° transverse positions of the speaker.

The sibilant /s/ is a broadband noise whose energy is mostly found in the frequency range above 4 kHz [4]. It is described as being produced by turbulent jet flow impinging on the upper and lower teeth [5], whereby the lips are also thought to play a role [6]. High-frequency sound propagation is governed not only by a plane-wave acoustic mode, but also by additional three-dimensional higher order modes, which contribute to both the acoustic field inside the vocal tract and the pressure pattern outside the vocal tract [7, 8]. Therefore, the acoustic field outside the vocal tract depends not only on the area function of the vocal tract, but also on the details of its three-dimensional geometry.

Moreover, the influence of the geometry of the vocal tract exit, *i.e.* the lip horn, on the acoustic behavior of the vowel vocal tract replicas was investigated using finite element simulations and experiments [9]. By comparing the replica with and without lips, it was found that the lip horn affected the frequency and quality of acoustic resonances and anti-resonances of the vocal tract. It was also suggested that the lip horn affects the pressure distribution downstream from the vocal tract. Since it was found that sibilant fricative /s/ exhibited the largest difference in the directivity pattern compared with those of vowels and other fricatives for human speakers [3], it is of interest to investigate the influence of the lip horn on the pressure distribution of sibilant /s/.

Therefore, in the current study, we experimentally study the potential effect of the lip horn on the pressure distribution outside the vocal tract of sibilant fricative /s/ using a vocal tract replica, whose lips can be removed from the upper and lower jaws without changing the position of the jaws. Since some previous studies on vocal tract models have used the replica without lips (e.g., for vowels [9], for fricatives [7]), we compare results of the replica with and without lips. In addition, using a replica instead of a human speaker allows measurement of the spatial pressure pattern in the near field with a higher spatial accuracy than the angle 15° [3]. Indeed a higher spatial accuracy is motivated

Received 3 April 2017,
accepted 15 November 2017.

since higher order modes associated with higher frequencies [7, 8] potentially result in a significant variation of the pressure pattern over a small spatial interval [10].

In this paper, the measurements with a single microphone mounted on a 3D positioning system with spatial accuracy of angle 2° in the near-field of the replica were compared to measurements with a spatial accuracy of angle 15° in the far-field. Moreover, the sound generated by an acoustic source positioned at the inlet of the replica was compared with the sound generated by supplying flow to the replica. With this comparison, we can study the influence of the sound source characteristics on the measured acoustic pressure distributions outside the vocal tract.

The measurement methodology is outlined in Section 2. Measured pressure patterns are presented in Section 3 and further discussed in Section 4. A conclusion is formulated in Section 5.

2. Methodology

2.1. Construction of the replica

Details of the method used to construct the vocal tract replica pronouncing sibilant /s/ are described by Nozaki *et al.* [11]. The vocal tract geometry was reconstructed from computed tomography (CT) images of a 32-year-old Japanese male subject with normal dentition (Angle Class I) without any speech disorder (self-report). During CT imaging, 512 sagittal slices of 512 pixel × 512 pixel (isotropic 0.1 × 0.1 × 0.1 mm^3 voxels) were obtained while the subject sustained the sibilant /s/ for 9.6 s in a seated position. There is no vowel context for the sustained /s/.

The replica consisted of a pharynx, upper and lower jaws, a tongue, and lips. The upper and lower jaws were produced using rapid prototyping (Zprinter, 3D systems; accuracy: ±0.1 mm). The pharynx, tongue, and lips were made of silicone resin (Wave Silicone, Wave Corp.). The lips were firmly attached to the upper and lower jaws so that there was no gap between jaws and lips. The inlet of the pharynx in the replica was positioned just above the base of the subject's epiglottis. The dimensions of the maximum constriction in the coronal plane is 8 mm by 1.25 mm. The distance between the constriction and tip of the upper teeth is 8 mm. It has been confirmed that this replica reproduced the subject's sibilant /s/ in the frequency range from 3 to 15 kHz [11].

A rectangular baffle was placed on the jaws or lips, as shown in Figure 1 to mimic the face. For the replica with lips, the baffle was positioned at the point where the lower and upper lips joined. For the replica without lips, the baffle was positioned at the same position as when the lips were present. The space between the baffle and canine teeth or lips was filled with modeling clay. The size of the baffle was changed depending on the measurement distance. The maximum aperture along the sagittal z-direction between the upper and lower lips was 5 mm. The largest aperture along the transverse y-dimension of the lip opening was 27 mm. For the case without lips, the largest aperture of the front teeth along the y-dimension was also 27 mm. The vocal tract length along the tongue surface (109 mm) was increased by 13 mm with the lower lip and by 12.5 mm with the upper lip.

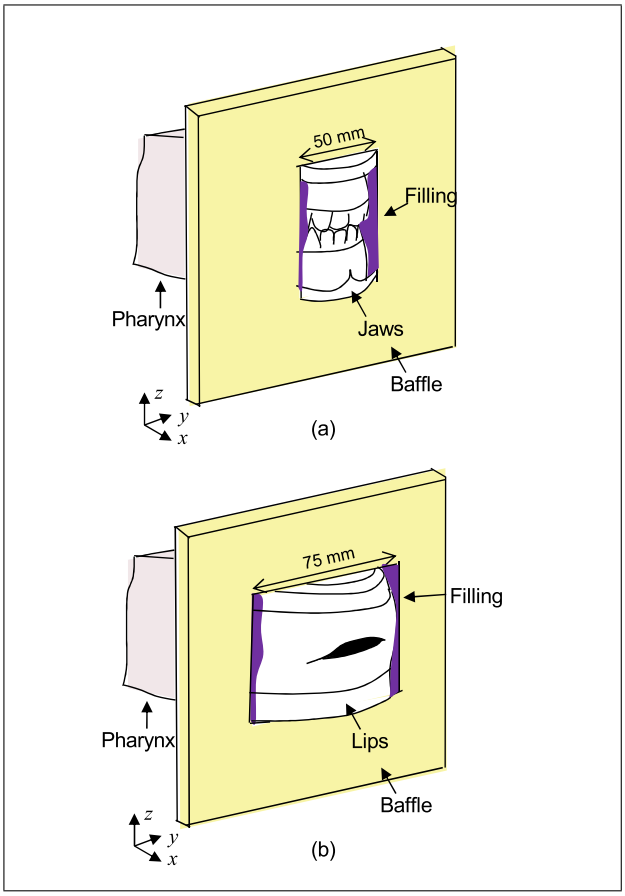

Figure 1. (Colour online) Replica with a rectangular baffle without lips (a) and with lips (b).

2.2. Measurement with acoustic source

The sound generated from a compression driver (SP-DYN-PRO2, Sphynx) positioned at the inlet of the pharynx was measured along two semi-circles of radius 4 cm (near-field) and radius 48 cm (far-field) from the lips. A compression driver is used instead of a loudspeaker in order to ensure sufficient acoustic energy in the frequency range of interest. The compression driver was connected to the inlet of the replica using a communication hole of 2-mm diameter as shown in Figure 2a. The replica was mounted near the inlet of a quasi-anechoic chamber (internal volume 7.45 m^3)[12] as schematized in Figure 3a for the near-field measurement and Figure 3b for the far-field measurement. The size of the baffle was changed from 36 × 36 cm for the near field measurement to 160 × 130 cm ($y \times z$) for the far-field measurement.

In the near-field, a single microphone probe with a probe length 25 mm (flat frequency response up to 14 kHz; type 4182, B&K) was mounted on a spatial 3D positioning system (PS35, OWIS; accuracy: ±100 μm). The tip of

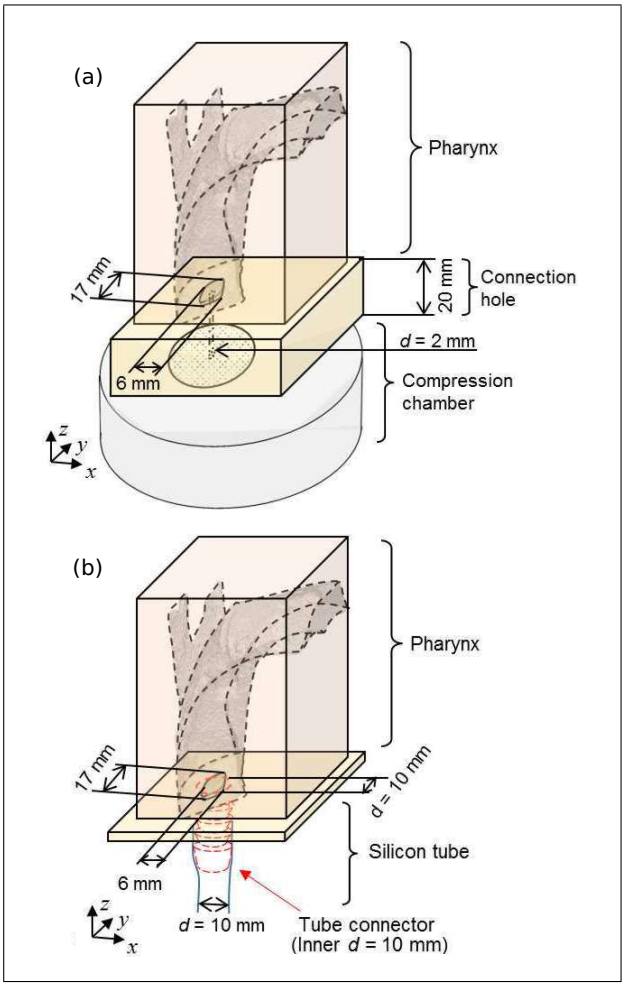

Figure 2. (Colour online) (a) Inlet geometry for the case with acoustic source. (b) Inlet geometry for the case with flow.

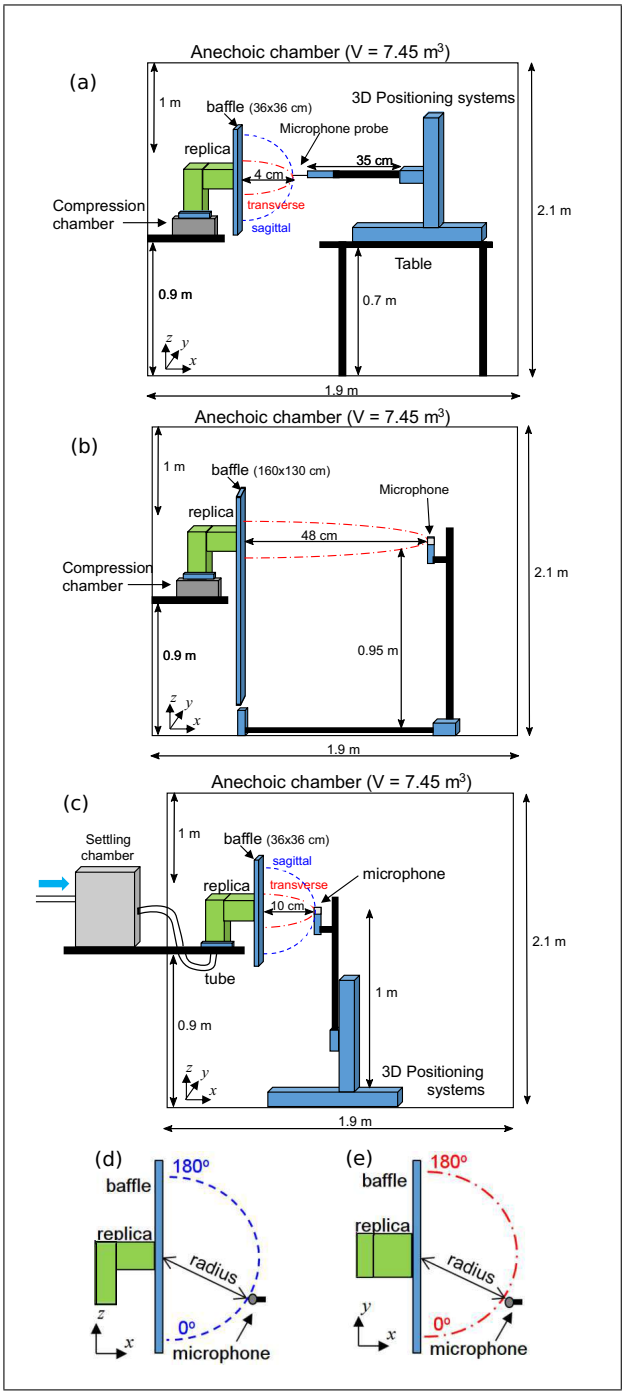

Figure 3. (Colour online) Illustration of the experimental setup used for pressure distribution measurements with acoustic source in near-field (a), in far-field (b) and with flow (c). The measurement positions in the sagittal and transverse planes are depicted in (d) and (e), respectively.

the probe was positioned along the transverse plane and sagittal plane at positions from 0° to 180° in steps of 2° as shown in Figure 3d and 3e. In the far-field, a single 1/2-inch microphone with flat frequency response up to 20 kHz (type 4192 and pre-conditioner type 5935L, B&K) was positioned at the same height as the replica with a rectangular bar (length: 1 m). The position of the microphone was shifted along the transverse plane (x-y plane) from 0° to 180° in steps of 15°. When the sound along the sagittal plane (x-z plane) of the replica was measured, the replica was tipped on its side so that the semi-circular transit of the microphone was in the replica's sagittal plane. Considering the wavelength of the generated sound, the minimum frequency of the far-field measurement at 48 cm is approximately 720 Hz.

At each microphone position, a linear sweep signal was amplified (A-807, Onkyo) and emitted by the compression driver in the frequency range of 2–15 kHz for 20 s. At each position, the microphone signal was recorded with a sampling frequency of 44.1 kHz using a data acquisition system with multiple input and output channels (NI PXI0MIO 16 XE, National Instruments). With the recorded signals, the power spectrum densities (PSDs) were calculated with 863 time segments of Fourier transforms of 1024 sample points (total time 20 s). The temperature in the quasi-anechoic room during the measurements ranged from 20.4 to 21.2 °C yielding a sound speed of 344.0 ± 0.3 m/s during the measurements.

Measured acoustic pressures are then characterized by considering the PSD amplitude extracted for each frequency. Since the amplitude of the sound emitted by the

loudspeaker depends on the frequency, measured values need to be normalized for each frequency. For the contour map (Figure 4 and 5 shown below), the extracted amplitudes were normalized by their spatial mean of the pressure pattern at each frequency. For the angular plot (Figure 6, 7, and 8 shown below), the extracted amplitudes were normalized by their maximum value of the pressure pattern at each frequency. This normalization removes the spurious influence of the sound source which can hinder interpretation of the results.

2.3. Measurement with flow

Air was supplied using a flow facility consisting of a compressor (GA7, Atlas Copco), a pressure regulator (type 11-818-987, Norgren), a manual valve, a mass-flow meter (model 4045, TSI), and a settling chamber ($40 \times 40 \times 50\,\mathrm{cm}^3$). The settling chamber was tapered with acoustic foam (SE50-AL-ML, Elastomeres Solutions) and equipped with flow straighteners in order to avoid acoustic resonances (due to the flow facility setup or settling chamber) and to homogenize the flow. Air issuing from the settling chamber was introduced to the replica through a silicone tube with a diameter of 1 cm and a length of 59 cm. The inlet geometry of the replica is depicted in Figure 2b. The turbulence level at the inlet of the replica was less than 3% [13]. Experiments were conducted at a flow rate of $40\,\mathrm{L{\cdot}min^{-1}}$, which corresponds to the subject's medium flow rate of /s/ in three effort levels, soft, medium and loud [14]. The flow rate was varied from 35 to $45\,\mathrm{L{\cdot}min^{-1}}$ while the subject sustained /s/ at the medium level. The corresponding Reynolds number is 5636 based on the characteristic dimension of the sibilant groove (the height of the maximum constriction 1.25 mm) and flow velocity at the groove. The size of the baffle is 36×36 cm.

A single 1/2-inch microphone (type 4192, B&K) was positioned along a semi-circle of radius 10 cm using the 3D positioning system (PS35, OWIS), as schematized in Figure 3c. The radius was increased compared to the near-field measurement with the acoustic sound source in order to prevent the impingement of the flow on the microphone. The spatial positioning system was placed on the floor of the acoustic chamber and covered with acoustic foam to minimize disturbances of the acoustic field. The microphone was attached to the positioning system with a bar (length: 1 m) and positioned along the transverse plane (x-y plane) and sagittal plane (x-z plane) from 0° to 180° in steps of 2° as shown in Figure 3d and 3e. Considering the wavelength, the minimum frequency of the far-field measurement at 10 cm is approximately 3440 Hz. At each position, the microphone signal was recorded for 2 s with a sampling frequency of 44.1 kHz using the data acquisition system. With the recorded signals, PSDs were calculated by time-averaging the Fourier transforms of 60 Hanning-windowed time segments of 1024 sample points with 30% overlap. To allow comparison between pressure patterns measured with and without flow, measured values were again normalized by the spatial mean or maximum amplitude for each frequency. The temperature in the quasi-anechoic room ranged from 18.7 to 20.9 °C yielding a sound speed of 343.5 ± 0.7 m/s during the measurements.

3. Results

Normalized acoustic pressure amplitudes of the sounds generated by the replica with and without lips along the transverse plane are mapped in Figure 4 for the case with acoustic source in near-field (a), (b), in far-field (c), (d), and for the case with flow (e), (f). The pressure distributions observed with and without lips were mainly changed above 5 kHz for all measurement conditions. The amplitudes at the angle around 90° were increased and the amplitudes near 0° and 180° decreased when the lips were present. The position of the maximum pressure amplitude was shifted from angle 0° to 140° above 12 kHz for the case with acoustic source.

Normalized acoustic pressure amplitudes of the sounds generated by the replica with and without lips along the sagittal plane are mapped in Figure 5 for the case with acoustic source in near-field (a), (b), in far-field (c), (d), and for the case with flow (e), (f). For the case without lips, the large trough at angles between 100° and 140° in the frequency range from 9 up to 10 kHz was observed for all measurement conditions. The amplitudes at the angle around 90° were increased and the amplitudes at the angle around 0° and 180° decreased above 5 kHz when the lips were present.

The acoustic pressure amplitudes measured with and without the lips at 6.1 kHz and 9.5 kHz are plotted in Figure 6 as a function of angle for the near-field measurement with acoustic source. The amplitudes in each measurement were normalized by the maximum value at each frequency. In the transverse plane, the amplitudes at the angle around 30° and 160° at 6.1 kHz decreased by 15 dB and 10 dB, respectively, when the lips were present. The amplitudes at the angle around 0° and 170° at 9.5 kHz decreased by 8 dB and 5 dB, respectively, when the lips were present. In the sagittal plane, the amplitudes at the angle around 0° and 150° at 6.1 kHz decreased by 7 dB and 10 dB, respectively, when the lips were present. The amplitudes at the angle around 20° and 110° at 9.5 kHz decreased by 10 dB and 15 dB, respectively, when the lips were present.

The acoustic pressure amplitudes measured with lips at 6.1 kHz and 9.5 kHz are plotted in Figure 7 as a function of angle for the near-field and far-field measurements with acoustic source. As before, the amplitudes in each measurement were normalized by the maximum value at each frequency. In the transverse plane, the amplitudes in far-field at the angle around 0° and 180° at 6.1 kHz were 10 dB larger than those in the near-field. The amplitudes at the angle around 0° and 180° at 9.5 kHz were 15 dB smaller than the amplitudes at the angle around 90° for both far-field and near-field. In the sagittal plane, the trough in amplitudes at the angle 150° was observed at 6.1 kHz for both far-field and near-field. The troughs in amplitudes at angles around 20° and 175° were observed at 9.5 kHz for both far-field and near-field.

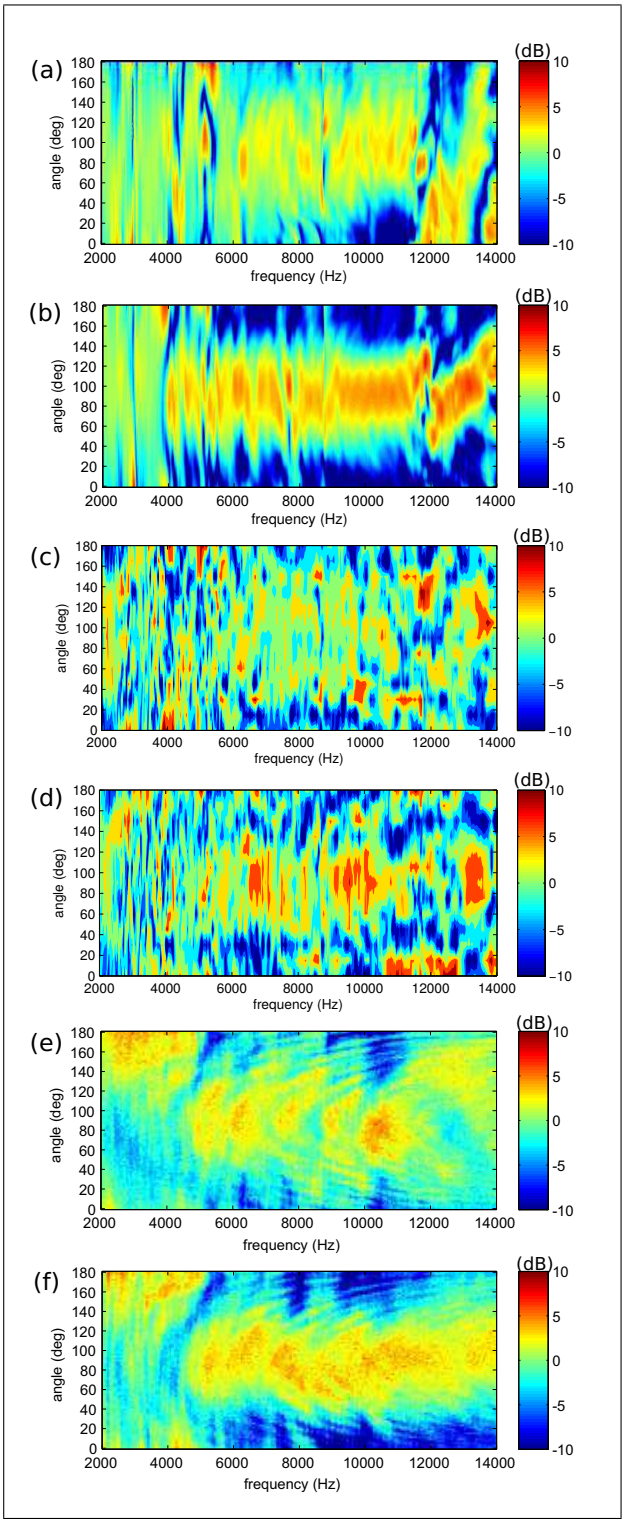

Figure 4. (Colour online) Normalized acoustic pressure amplitudes measured along the transverse plane for the case with acoustic source in near-field (radius 4 cm, every 2°) without lips (a), with lips (b), in far-field (radius 48 cm, every 15°) without lips (c), with lips (d), and for the case with flow (radius 10 cm, every 2°) without lips (e), with lips (f).

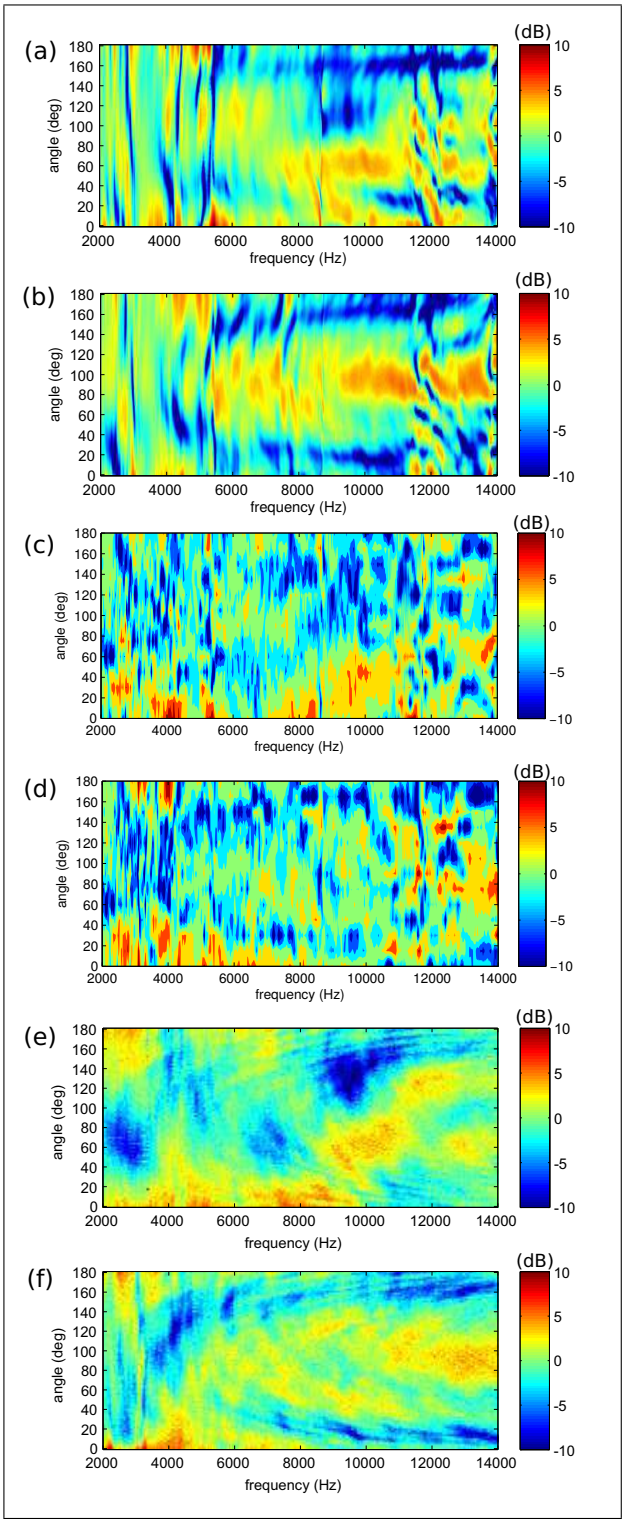

Figure 5. (Colour online) Normalized acoustic pressure amplitudes measured along the sagittal plane for the case with acoustic source in near-field (radius 4 cm, every 2°) without lips (a), with lips (b), in far-field (radius 48 cm, every 15°) without lips (c), with lips (d), and for the case with flow (radius 10 cm, every 2°) without lips (e), with lips (f).

The acoustic pressure amplitudes measured with lips at 6.1 kHz and 9.5 kHz are plotted in Figure 8 as a function of angle for the case with acoustic source and flow. As before, the amplitudes in each measurement were normalized by the maximum value at each frequency. In the transverse plane, the amplitudes measured with flow at the an-

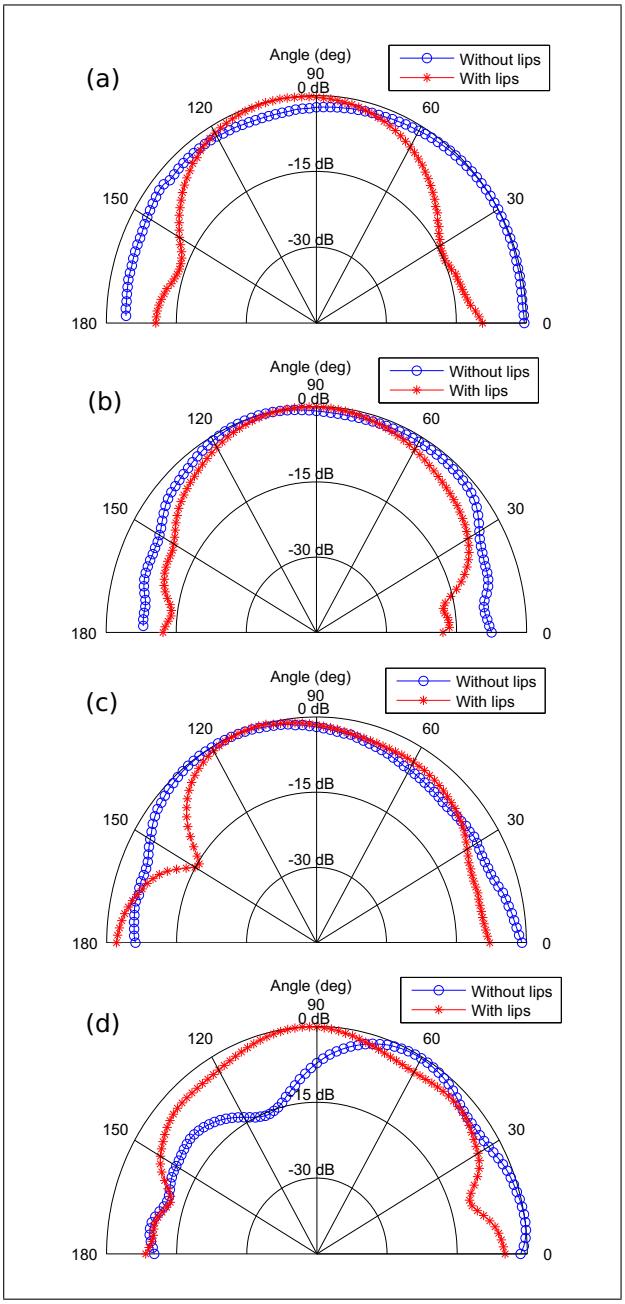

Figure 6. (Colour online) Normalized acoustic pressure amplitudes as a function of angle for the near-field (radius 4 cm) measurement with acoustic source. Measurements along the transverse plane are plotted in (a) at 6.1 kHz, and (b) at 9.5 kHz. Measurements along the sagittal plane are plotted in (c) at 6.1 kHz, and (d) at 9.5 kHz.

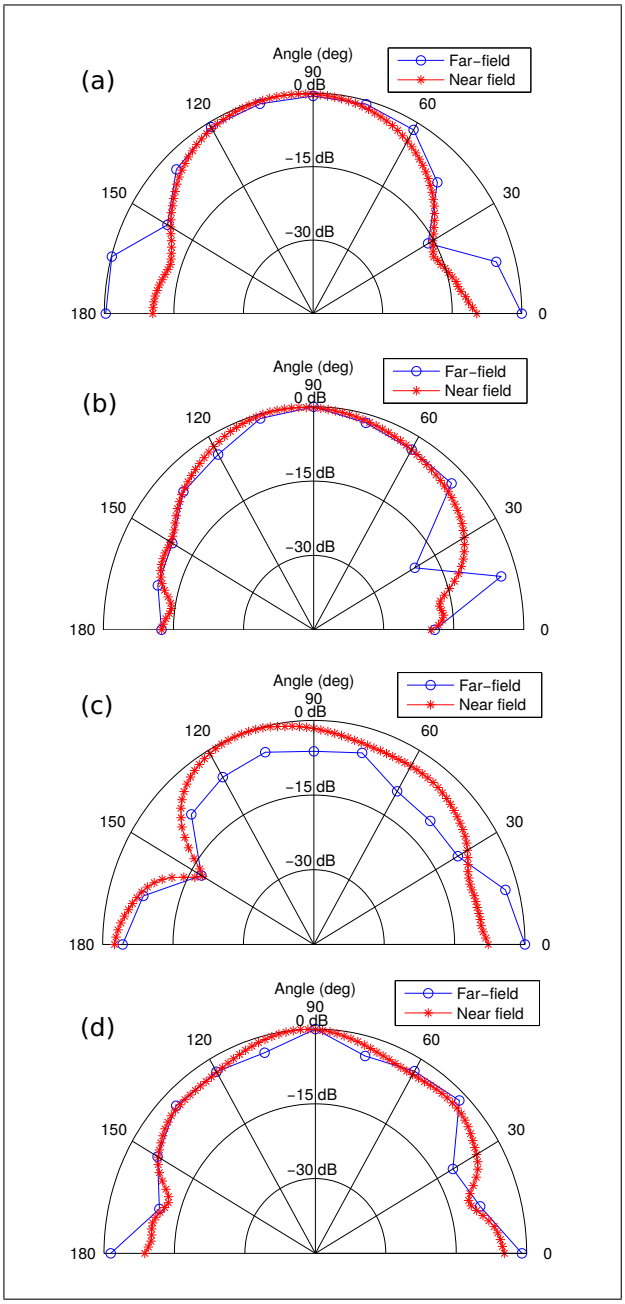

Figure 7. (Colour online) Normalized acoustic pressure amplitudes as a function of angle for the far-field (radius 48 cm) and near-field (radius 4 cm) measurements with acoustic source and lips. Measurements along the transverse plane are plotted at (a) 6.1 kHz, and (b) 9.5 kHz. Measurements along the sagittal plane are plotted at (c) 6.1 kHz, and (d) 9.5 kHz.

gle 30° and 160° at 6.1 kHz were 5 dB and 10 dB larger, respectively, than those measured with acoustic source. The amplitudes at angles around 0° and 180° at 9.5 kHz were 15 dB smaller than that at angles around 0° for both the flow case and the acoustic source case. In the sagittal plane, the amplitudes measured with flow at the angle 15° and 150° at 6.1 kHz were 7 dB larger than those measured with acoustic source. The troughs in amplitude at the angle around 20° and 175° were observed at 9.5 kHz for both cases, *i.e.* with acoustic source and with air flow.

4. Discussion

The pressure distribution measurements in the transverse and sagittal planes showed that the pressure amplitudes at angles associated with the center of the lips (*i.e.*, the angles around 90° in both planes) increased up to 15 dB when the lips were present in the frequency range above 5 kHz. This increase was observed for all measurement conditions (*i.e.*, near-field and far-field with the acoustic source or with flow supply). Far-field pressure fields of a

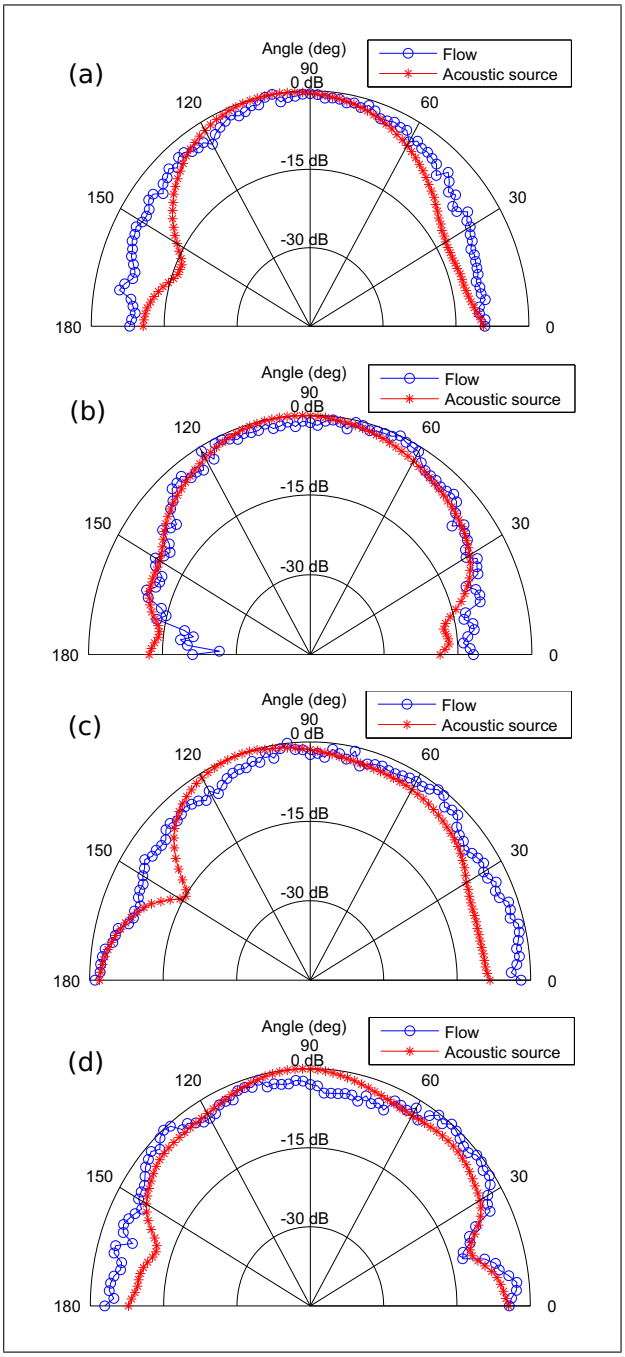

Figure 8. (Colour online) Normalized acoustic pressure amplitudes as a function of angle for the measurements with acoustic source (radius 4 cm) and flow (radius 10 cm). Both plots are for the case with lips. The measurement along the transverse plane are plotted at (a) 6.1 kHz, and (b) 9.5 kHz. The measurement along the sagittal plane are plotted at (c) 6.1 kHz, and (d) 9.5 kHz.

concentric rigid two-tube simplification of vowel /ɑ/ vocal tract with an infinite baffle (no lips) [10], showed that the amplitude at 90° was larger than those at 0° and 180° above 6.5 kHz, and the maximum difference of amplitudes between the center (90°) and side regions (0° and 180°) was approximately 10 dB in the frequency range from 2 to 10 kHz. The maximum difference in the amplitude for the replica of /s/ was 15 dB for this frequency range (2 to 10 kHz), and these results indicate that the lip horn plays a role to enhance the directivity at the center compared to the model of /ɑ/. This enhanced directivity in front of the mouth was also observed in the previous measurements of sibilant /s/ on human speakers [3] and might therefore be partly due to the lip horn. It is of interest to further investigate the effect of the lips on other sounds in order to investigate the role of the lip horn for the sound radiation. Another potential parameter for the future study is the geometry of the lip horn (*e.g.* parameters for the curvature and protrusion of the radiating surface).

Directivity measurements conducted with an eccentric two tube simplification of /ɑ/ without lips showed that complex directivity patterns, with changes in directivity within short frequency and angle intervals, occur in the frequency range above 6.5 kHz [10]. The influence of the lips on the transfer function of the /ɑ/ vocal tract was mainly observed above 5.5 kHz [9]. In this study, complex pressure patterns were observed with and without lips for frequencies above 4 kHz (normalized pressure amplitude differences up to 10 dB), which is significantly lower than that found in the vocal tract of /ɑ/. This suggests that the higher order modes of sibilant /s/ affect the pressure pattern at lower frequencies than that observed for vowels. This is in agreement with the argument that the higher order modes affect the pressure pattern below the first cut-on frequency, and plane-wave theory holds for frequencies below 4 kHz for the vocal tract geometries of sibilant fricatives [7]. Further acoustic modeling of wave propagation through the replica's geometry is needed in order to further examine the effect of higher order modes in sibilant fricatives.

A similar tendency was observed between the near-field and far-field measurements, although the resolution in the far-field (15°) was lower than that in the near-field (2°). This indicates that more precise measurement of the directivity pattern compared to the far-field measurement was achieved by using the 3D positioning system in the near field of the vocal tract. This result encourages a future development of a setup enabling a precise measurement of the directivity pattern in the far-field in order to confirm the current findings using other replicas and eventually on human speakers to investigate the perceptual relevance of the current findings.

The comparison between the case with acoustic source and flow revealed a similar tendency in both the transverse and sagittal plane. In particular, similar pressure distributions were observed in the frequency range from 7 to 10 kHz, which coincides with the frequency range of the highest acoustic energy observed on replica's sibilant /s/ [11]. When the flow was supplied to the replica, the noise source was probably generated downstream from the sibilant groove, *i.e.* around the incisors and lips. Nevertheless, similar pressure distribution patterns were observed for the different sound source positions, *i.e.* at the inlet of the pharynx or downstream from the sibilant groove. This indicates that the pressure pattern outside the vocal tract

of sibilant /s/ is less affected by the position of the sound source than by the vocal tract geometry. It is of interest to confirm this finding for other fricatives since usage of an acoustic source allows a detailed spatial measurement of the acoustic pattern inside and outside of the vocal tract geometry which is difficult to achieve in the presence of flow.

5. Conclusion

In the current study, acoustic pressure distribution patterns were measured on a vocal tract replica of sibilant /s/ with and without lips. It was found that complex pressure patterns with differences in amplitude of approximately 10 dB occur with and without lips for frequencies above 4 kHz. The lip horn enhances the pressure amplitude up to 15 dB at the center of the lips in both transverse and sagittal plane in the frequency range above 5 kHz. These tendencies were observed in the near-field and far-field measurements with the acoustic source, and in the measurements with flow supply. The comparison between the near-field and far-field measurements showed that more precise directivity pattern can be achieved by the near-field measurement compared to the far-field measurement. The comparison between the acoustic source and flow source showed that the pressure distribution pattern is affected by the vocal tract geometry rather than by the source characteristics.

The presented experimental results motivate further studies involving spatially detailed directivity pattern measurements for different phonemes using the vocal tract replicas in combination with an acoustic source in order to further study the effect of the lip horn as well as to study the acoustic pressure patterns for different phoneme geometries. Furthermore, the perceptual relevance of these findings needs to be further investigated.

Acknowledgement

This work was partly supported by ArtSpeech Project (ANR-15-CE23-0024), JSPS Grant-in-Aid for JSPS Research Fellows (JP15J004130), MEXT as "Priority Issue on Post-K computer" (Project ID: hp160218), and the Program for Leading Graduate Schools of MEXT (Humanware Innovation Program). We acknowledge Dr. Rémi Blandin for his contribution to the experiments.

References

[1] H. K. Dunn, D. W. Farnsworth: Exploration of pressure field around the human head during speech. J. Acoust. Soc. Am. **10** (1939) 184–199.

[2] D. Cabrera, P. J. Davis, A. Connolly: Long-term horizontal vocal directivity of opera singers: effects of singing projection and acoustic environment. J. Voice **25** (2011) e291–e303.

[3] B. B. Monson, E. J. Hunter, B. H. Story: Horizontal directivity of low- and high-frequency energy in speech and singing. J. Acoust. Soc. Am. **132** (2012) 433–441.

[4] L. Jesus, C. Shadle: A parametric study of the spectral characteristics of European Portuguese fricatives. J. Phon. **30** (2002) 437–464.

[5] C. H. Shadle: The effect of geometry on source mechanisms of fricative consonants. J. Phon. **19** (1991) 409–424.

[6] C. H. Shadle, C. Scully: An articulatory-acoustic-aerodynamic analysis of [s] in VCV sequences. J. Phon. **23** (1995) 53–66.

[7] K. Motoki: A parametric method of computing acoustic characteristics of simplified three-dimensional vocal-tract model with wall impedance. Acoust. Sci. Technol. **34** (2013) 113–122.

[8] R. Blandin, M. Arnela, R. Laboissière, X. Pelorson, O. Guasch, A. Van Hirtum, X. Laval: Effects of higher order propagation modes in vocal tract like geometries. J. Acoust. Soc. Am. **137** (2015) 832–843.

[9] M. Arnela, R. Blandin, S. Dabbaghchian, O. Guasch, F. Alias, X. Pelorson, A. Van Hirtum, O. Engwall: Influence of lips on the production of vowels based on finite element simulations and experiments. J. Acoust. Soc. Am. **139** (2016) 2852–2859.

[10] R. Blandin, A. Van Hirtum, X. Pelorson, R. Laboissiere: Influence of higher order acoustical propagation modes on variable section waveguide directivity: application to vowel [a]. Acta Acust united Ac **102** (2016) 1–12.

[11] K. Nozaki, T. Yoshinaga, S. Wada: Sibilant /s/ simulator based on computed tomography images and dental casts. J. Dent. Res. **93** (2014) 207–11.

[12] A. Van Hirtum, Y. Fujiso: Insulation room for aero-acoustic experiments at moderate Reynolds and low Mach numbers. Appl. Acoust. **73** (2012) 72–77.

[13] A. Van Hirtum, Y. Fujiso, K. Nozaki: The role of initial flow conditions for sibilant fricative production J. Acoust. Soc. Am. **136** (2014) 2922–2925.

[14] Y. Fujiso, K. Nozaki, A. Van Hirtum: Estimation of minimum oral tract constriction area in sibilant fricatives from aerodynamic data. J. Acoust. Soc. Am. **138** (2015) EL20–EL25.